Eur. Phys. J. D **11**, 327–334 (2000)

THE EUROPEAN PHYSICAL JOURNAL D

EDP Sciences

Resonance effects in nonlinear lattices

M. Leo[1], R.A. Leo[1], A. Scarsella[2], and G. Soliani[1,a]

[1] Dipartimento di Fisica dell'Università, 73100 Lecce, Italy
[2] Liceo Scientifico "L. da Vinci", Maglie, 73100 Lecce, Italy

Received 16 August 1999 and Received in final form 3 February 2000

Abstract. We study a class of one-dimensional nonlinear lattices with nearest-neighbour interactions described by a potential of the binomial type. This potential contains a free parameter which can be chosen to reproduce a variety of models, such as the Toda, the Fermi-Pasta-Ulam and the Coulomb-like lattices. Carrying out essentially numerical experiments, the effects of soliton propagation on a lattice with defects are investigated. In particular, the properties of the localized mode, generated by the propagation of the soliton through the defect, are discussed with respect to the defect mass and the potential parameter, in the light of a simple theoretical model. Furthermore, an interesting phenomenon is observed: the amplitude of the speed of the mass defect shows a sequel of resonance peaks in terms of the mass defect. The positions of these peaks appear to be independent of the potential parameter.

PACS. 63.10.+a General theory – 05.45.-a Nonlinear dynamics and nonlinear dynamical systems – 05.45.Yv Solitons

1 Introduction

In the study of discrete dynamical systems with nearest-neighbour interactions, generally the absence of integrability properties compels one to exploit suitable approximations or to integrate numerically the equations of motion. Usually the continuous approximation of a given lattice leads to a nonlinear partial differential equation whose solutions can be employed, in theory, as initial conditions for solving *via* numerical procedures the original discrete equations. On the other hand, continuous limits of lattice systems can be considered as phenomenological models with a proper identity and, apart from some lucky circumstances, the intrinsic properties of lattice systems and their corresponding field versions are not always preserved. The problem becomes much more complicated when lattices with defects are studied. In these cases the discreteness of the lattice cannot be ignored when certain effects involving, for example, soliton dynamics [1] and excitation of localized modes are dealt with [9].

The main purpose of this paper is just to analyse the interaction between solitons and defects in a one-dimensional lattice in case the nonlinear character of the interaction is dominant, in such a way that both the effects of the discreteness and the strong nonlinearity can be evidenced.

We investigate a wide class of nonlinear atomic chains whose equations of motion come from a potential of the "binomial" type introduced by some of us a long time ago [2]. This model, described in Section 2, contains a free parameter γ which allows us to cover several special cases of physical interest, running from the Toda potential ($\gamma \to \infty$), to the Fermi-Pasta-Ulam ($\gamma = 3$) and the Coulomb-like potential ($\gamma = -1$). The binomial potential includes the linear case as well, which is reproduced for $\gamma = 2$.

Section 3 is devoted to the Cauchy problem for the equations of motion of the lattice. In the long wave approximation of the discrete model, we obtain two solutions of the equations of motion of the supersonic and subsonic travelling wave type. In the supersonic case, independently of the value of the parameter γ, under certain conditions a solitary wave propagates without ripples. This solution can be interpreted as a soliton-like pulse. At the increasing of the supersonic character of the initial condition, a sequence of ripples appears around the main travelling wave, due to the discreteness of the lattice.

Using the supersonic solution (a kink soliton) as initial condition, in Section 4 we consider the lattice in presence of a defect mass. We carry out computer experiments for different choices of the parameter γ, including the Toda case. Independently of the kind of binomial potential, the interaction of the kink with the defect excites a localized mode which turns out to decay exponentially in the space variable. This localized motion of the defect is harmonic with a period depending on the mass m_{d} of the defect and on γ.

Moreover, a notable phenomenon appears. Precisely, in the plot of the amplitude of the mass defect speed in terms of m_{d}, a sequel of resonance peaks is present.

Concerning the analysis of the periods of oscillations as functions of m_{d} and γ we resort to a simple model

[a] e-mail: soliani@le.infn.it

which explains fairly the numerical results. On the contrary, we have not be able to find any satisfactory theoretical explanation for the presence of resonance peaks in the amplitude of the mass defect speed. A possible reason of this is due to the fact that the classical methods of linear approximation of the defect-soliton interaction are not adequate when strong nonlinearity behaviours occur. The linear approximation allows one to explain only the main peak of resonance, as it is shown in reference [7].

In Section 5 the analysis of Section 4 is extended to the case of a lattice with two defective atoms. In this case we obtain again the appearance of multi-peak resonance phenomena, which are widely discussed. Finally, in Section 6 some concluding remarks are reported.

2 The model

Let us consider a one-dimensional chain of atoms interacting through the nearest-neighbour potential $\phi(y_{n+1}-y_n)$, where y_n denotes the displacement of the n atom from its equilibrium position. The system is described by the Hamiltonian

$$H=\sum_{n=1}^{N}\frac{1}{2}m_n\dot{y}_n^2+\sum_{n=1}^{N-1}\phi(y_{n+1}-y_n). \tag{1}$$

Here we deal with some special cases of the potential of the binomial type

$$\phi(r_n)=\frac{a}{b}\left[\left(1+\frac{b}{\gamma}r_n\right)^{\gamma}-(1+br_n)\right], \tag{2}$$

where $r_n=y_{n+1}-y_n$, γ is a real parameter, and a, b are constants characterizing the force and length scale, respectively (if $ab>0$, then $\gamma<0$ or $\gamma>1$; if $ab<0$, $0<\gamma<1$).

The equations of motion for the atoms of the lattice, *i.e.*

$$m_n\ddot{y}_n=f_n-f_{n-1}\quad(n=2,...,N-1), \tag{3}$$

where

$$f_n=a\left[\left(1+\frac{b}{\gamma}r_n\right)^{\gamma-1}\right], \tag{4}$$

are derived from

$$\frac{\mathrm{d}}{\mathrm{dt}}\frac{\partial H}{\partial\dot{y}_n}=-\frac{\partial H}{\partial y_n} \tag{5}$$

with $n=1,...,N$.

Equations (3) can be written in the compact form

$$\ddot{y}_n=\omega_n^2\sum_{i=1}^{p(\gamma)}\alpha_i(\gamma)(r_n^i-r_{n-1}^i) \tag{6}$$

where

$$\omega_n^2=\frac{k}{m_n}=\frac{ab}{m_n}\frac{\gamma-1}{\gamma} \tag{7}$$

k being the constant of the springs, and

$$p(\gamma)=\begin{cases}\gamma-1, & \gamma\in\mathbf{N}\\ +\infty, & \gamma\in\mathbf{R}-\mathbf{N}\end{cases} \tag{8}$$

with

$$\alpha_i(\gamma)=\begin{cases}1, & i=1\\ b^{i-1}\prod_{l=2}^{i}\frac{\gamma-l}{l\gamma}, & 1<i\le p(\gamma).\end{cases} \tag{9}$$

3 The Cauchy problem

To solve the Cauchy problem for equations (3), we have considered a continuous approximation of this, so that solutions of the resulting equation can be used as initial conditions for equations (3) in our numerical simulations.

To this aim, let us deal with the expansion in Taylor's series of $y_{n\pm1}$, namely

$$y_{n\pm1}=y_n\pm h\frac{\partial y_n}{\partial x}+\frac{h^2}{2!}\frac{\partial^2 y_n}{\partial x^2}\pm\frac{h^3}{3!}\frac{\partial^3 y_n}{\partial x^3}+..., \tag{10}$$

where $x=nh$, and h is the space distance between the atoms of the lattice at rest. If y_n is considered as a function of x and t, substitution from (10) into (3) yields

$$y_{tt}=c^2\left(y_{xx}+\frac{h^2}{12}y_{xxxx}\right)\left[1+2h\alpha_2\left(y_x+\frac{h^2}{6}y_{xxx}\right)+3h^2\alpha_3\left(y_x^2+\frac{h^2}{12}y_{xx}^2+\frac{h^3}{3}y_xy_{xxxx}\right)+...\right] \tag{11}$$

where $c^2=h^2k/m$, $y_x=\partial y/\partial x$, $y_t=\partial y/\partial t$, etc.

If we restrict ourselves to take into account in (11) only the terms up to the second order in h, we obtain

$$y_{tt}=c^2\left[\left(1+2h\alpha_2y_x+3h^2\alpha_3y_x^2\right)y_{xx}+\frac{h^2}{12}y_{xxxx}\right]. \tag{12}$$

We remark that equation (12) is of physical relevance. For example, it appears in the study of heat pulses propagation in solids [3]. We observe that the coefficients α_2 and α_3 depend on the parameter γ involved in the potential (2). Now we look for a solution to equation (12) of the travelling supersonic wave type

$$y=y(x-vt)=y(\chi), \tag{13}$$

where v ($v>c$) is a constant (the speed of the wave).

Inserting (13) into (12), we obtain

$$(\lambda-1)y_{\chi\chi}-2h\alpha_2y_\chi y_{\chi\chi}-3h^2\alpha_3y_\chi^2y_{\chi\chi}-\frac{h^2}{12}y_{\chi\chi\chi\chi}=0, \tag{14}$$

where $\lambda=v^2/c^2$, and $y_\chi=\mathrm{d}y/\mathrm{d}\chi$, and so on.

With a suitable choice of the constants of integration, equation (14) provides the solution

$$y(x,t) = \frac{2}{A\sqrt{D}} \arctan \frac{B+\mathrm{e}^{A(x-vt-\chi_0)}}{2\sqrt{D}}, \tag{15}$$

$$\dot{y}(x,t) = -v \frac{\mathrm{e}^{A(x-vt-\chi_0)}}{D+\left[\dfrac{B+\mathrm{e}^{A(x-vt-\chi_0)}}{2}\right]^2}, \tag{16}$$

where $A = \sqrt{12(\lambda-1)}/h$, $B = 2\alpha_2 h/3(\lambda-1)$, $D = \alpha_3 h^2/2(\lambda-1)$, and χ_0 is a constant. The quantity (15) represents a solution of the solitary wave kind, propagating with a velocity v, whose amplitude and width are characterized by the parameters A, B and D.

In the case of subsonic speeds ($v < c$), *i.e.* for $\lambda < 1$, equation (14) affords the solution

$$y(x,t) = -\frac{2}{A\sqrt{D}} \times \left\{ \arctan \frac{B \tan \frac{A(x-vt-x_0)}{2} - \sqrt{B^2-4D}}{2\sqrt{D}} + n\pi \right\}$$

if $A(x-vt-x_0)/2 \in ((n-1/2)\pi, (n+1/2)\pi)$, $n \in \mathbf{Z}$, where $A = \sqrt{12(1-\lambda)}/h$, $B = 2\alpha_2 h/3(1-\lambda)$, $D = \alpha_3 h^2/2(1-\lambda)$, and $B^2 - 4D > 0$. The last condition can be expressed as

$$\frac{2\gamma-7}{3(\gamma-3)} < \lambda < 1,$$

in terms of γ, where $\gamma < 2$ or $\gamma > 7/2$.

We notice that the kind of solutions obtained for $\lambda < 1$ cannot be exploited as initial condition to solve the Cauchy problem for the equations of motion (3). This happens because $y(x,t)$ is divergent asymptotically.

The functions (15, 16) have been used as initial conditions to determine numerical solutions to equations (3). In doing so, we have applied a bilinear symplectic algorithm of the third order, which has been adapted from an algorithm employed previously by Casetti [4]. Such a recipe allows us to obtain a control of the total energy E of the lattice, which ensures a relative error $\Delta E/E < 10^{-6}$. In our numerical calculations, we have considered a lattice with 66 atoms, the first and the last of which are fixed. The integration time step Δt comprises values ranging from 0.1 to 0.005. The last value is approximately 10^{-3} times the period of oscillation of the atoms in the harmonic case (see (7) for $\gamma = 2$). The time length of integration in all the simulations covers about 40 periods of these harmonic oscillations (7×10^4 time steps). Concerning the choice of the number of atoms in the lattice, we have performed several numerical integrations with a number of atoms greater than 66, until 150, obtaining essentially the same results. The numerical simulations have been performed by choosing $a = b = h = m_n = 1$ and $\chi_0 = 5$ for any atom of the lattice. The remaining parameters, α_2, α_3 and c, are defined in correspondence of the choice of the potential (2), *i.e.* for a fixed γ. Then the only free parameter is $\lambda = v^2/c^2$, in terms of which we have studied the behaviour of the solitary wave travelling in the lattice.

From the analysis of the numerical data obtained by us emerges that, independently of γ, for values of $\lambda > 1$ slightly different from 1, in the lattice a solitary wave propagates which preserves its shape. The profile of this wave remains unaltered in time also during the many reflections on the atoms situated at the fixed ends of the lattice, and no ripples are present. In other words, in this case the solitary wave behaves as a soliton. However, the increasing of λ produces a growth of the amplitude of the solitary wave, while its profile becomes narrower. These effects give rise, in the solutions of equations (3), to a sequence of ripples, which propagate in the lattice as dispersive waves with speeds lower than the speed of the principal pulse. However, at least up to values of $\lambda \cong 5$, the main pulse is preserved for a long time, notwithstanding the occurrence of frequent interactions with the ripples, which "invade" the lattice owing to the chosen boundary conditions.

Subsequently, we have examined the space configuration of the atoms for different values of time.

We note that the atoms collided by the solitonic pulse suffer damping oscillations caused by the ripples.

Such oscillations, which are essentially absent for $\lambda \cong 1$, are due to the fact that for $\lambda \gg 1$, the main wave begins to "see" the discreteness of the lattice. In practice, the dispersive component inside equations (3) cannot be longer neglected and the solution found within the continuous approximation does not hold anymore for the original (discrete) equations of motion. In the case of some special potentials, these phenomena have been already revealed [5,6].

4 Lattice with a mass defect

We have investigated the lattice containing an atom with mass $m_\mathrm{d} < m$, where $m = 1$ is the mass of the remaining atoms [7,8]. Our study concerns the analysis of the amplitude and the period of the oscillations of the defected atom after its collision with the solitonic pulse (15), in terms of its mass m_d. We have chosen values of m_d such that $0 < m_\mathrm{d} < 1$. The defect has been located at the site 54. This choice is motivated by the fact that, for the value of λ in correspondence of which we have carried out mostly our numerical simulations ($\lambda = 2.5$), the ripples propagating at a speed less than the speed of the main solitonic pulse, arrive at the site 54 only after that through this the pulse reflected by the fixed atom ($n = 66$) is passed. Hence, such ripples do not induce on the atom 54 spurious oscillations, at least within the time interval in which we are interested in the observation of the defected atom. The extremes of such an interval are just the time in which the direct pulse reaches the site $n = 54$, and the time in which this pulse comes back to this site after its reflection at $n = 66$.

These computer experiments have been performed for potentials corresponding to different values of γ (see (2)). In particular, we have analysed the periods of the oscillations induced on the defect in terms of m_d. We have found that the motion of the defect is harmonic with a period depending on m_d and γ. This behaviour is quite

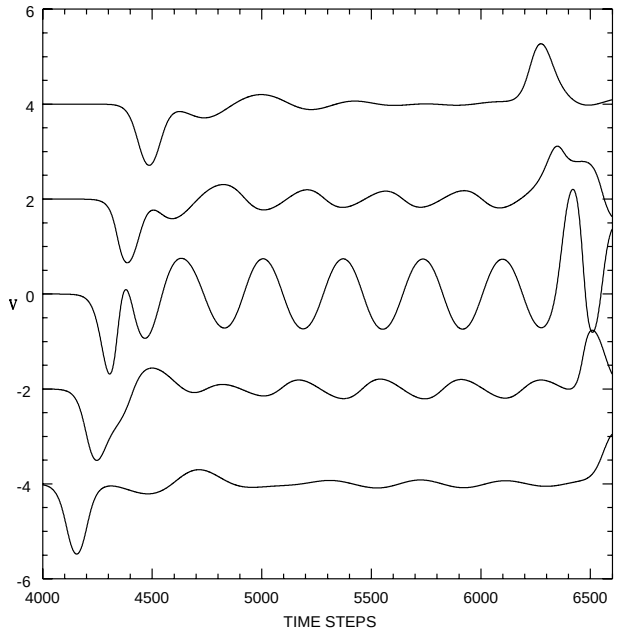

Fig. 1. Evolution in time ($n\Delta t$) of the speeds of the defect and their nearest-neighbour atoms (sites 52-56), in the case $\gamma = -1$ ($\Delta t = 0.005, m_{\rm d} = 0.40$). To make clearer the plot, the speeds relative to the sites 52, 53, 55, 56 have been shifted of -4, -2, $+2$, $+4$, respectively.

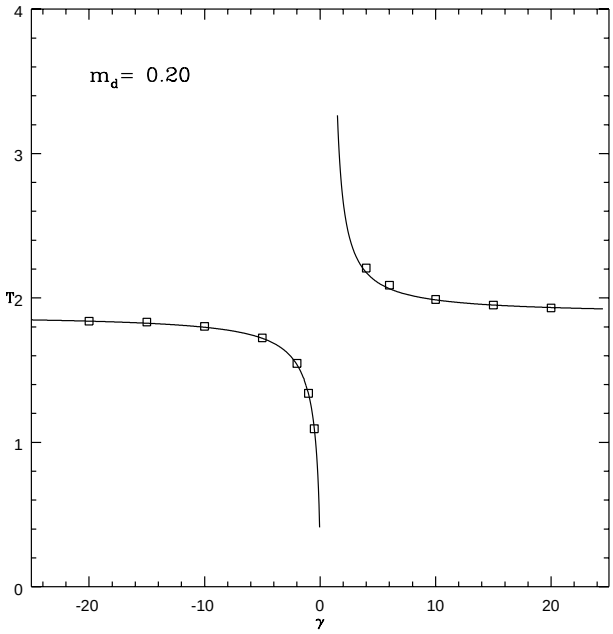

Fig. 2. Comparison between numerical experiments and the theoretical prediction (21) of the period of oscillation of the defect *vs.* γ for $m_{\rm d} = 0.2$.

reasonable, since the interaction of the kink with the defect excites, in the lattice, a localized mode which turns out to decay exponentially in the space variable.

In Figure 1 the speeds of the atoms immediately closed to the defect are reported *vs.* the time variable.

As one can see, the oscillations generated by the kink on the particles are of the asymmetric type, with a phase difference between two adjacent atoms approximately equal to π.

One can solve exactly the impurity mode problem, by noting that outside the strongly nonlinear regime, in the part of the chain covered by the soliton, the atomic lattice vibrates with standard small amplitude oscillations. In this harmonic frame, we have linearized the equations of motion (3), which become

$$m_n \ddot{y}_n = \frac{\gamma - 1}{\gamma}(y_{n+1} - 2y_n + y_{n-1}), \tag{17}$$

where $m_n = m_{\rm d}$, the defect mass, for $n = n_0$, and $m_n = 1$ for $n \neq n_0$.

We look for solutions of the type

$$y_n = A \exp\left(-\frac{\mid n - n_0 \mid}{L}\right) \exp(\mathrm{j}\phi_n) \exp(-\mathrm{j}\omega t) \tag{18}$$

where L characterizes the exponential decay of the localized mode. We assume $\phi_{n_0} = 0$ and $\phi_{n_0 \pm k} = \pm k\pi$. Inserting (18) into (17), for $n = n_0$ we obtain

$$-m_{\rm d}\omega^2 = \frac{\gamma - 1}{\gamma}\left[\exp\left(-\frac{1}{L}\right)\exp(\mathrm{j}\pi) - 2 + \exp\left(-\frac{1}{L}\right)\exp(-\mathrm{j}\pi)\right]$$

from which

$$\exp\left(-\frac{1}{L}\right) = \frac{\gamma}{2(\gamma - 1)} m_{\rm d}\omega^2 - 1. \tag{19}$$

For $n = n_0 + 1$, equations (17, 18) give

$$\omega^2 = \frac{\gamma - 1}{\gamma}\left[\exp\left(-\frac{1}{L}\right) + 2 + \exp\left(\frac{1}{L}\right)\right]. \tag{20}$$

By virtue of (19) and (20), we get

$$\omega = 2\sqrt{\frac{\gamma - 1}{\gamma}\frac{1}{m_{\rm d}(2 - m_{\rm d})}},$$

and

$$T = \frac{2\pi}{\omega} = \pi\sqrt{\frac{\gamma}{\gamma - 1} m_{\rm d}(2 - m_{\rm d})}. \tag{21}$$

In Figures 2–4 we plot the experimental data for T, obtained by integrating numerically equations (3), and compare these results with the theoretical behaviour predicted by (21), keeping the mass $m_{\rm d}$ fixed and varying the parameter γ.

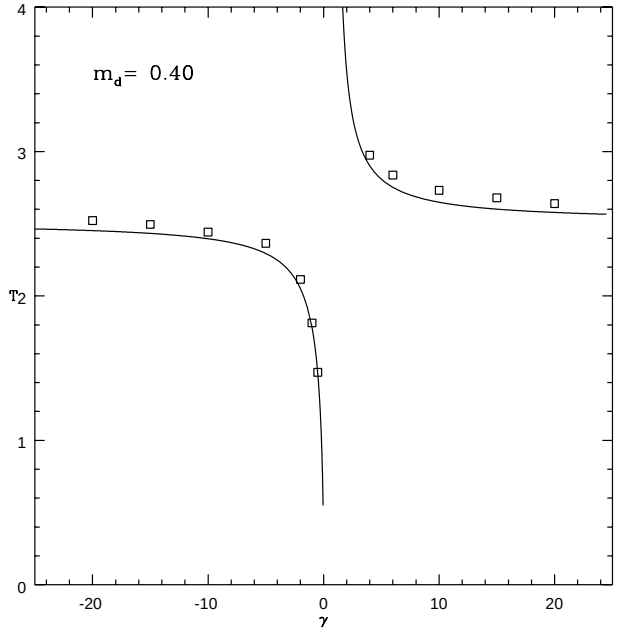

Fig. 3. As in Figure 2, but where now $m_{\rm d} = 0.4$.

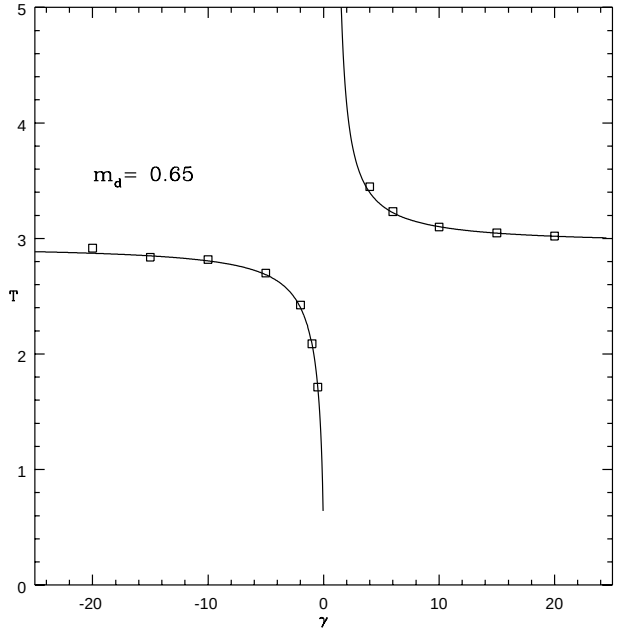

Fig. 4. As in Figure 2, but where now $m_{\rm d} = 0.65$.

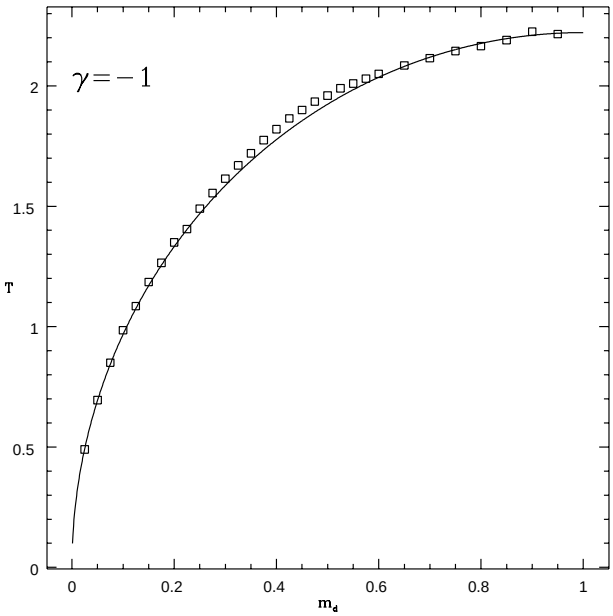

Fig. 5. Comparison between numerical experiments and the theoretical prediction (21) of the period of oscillation of the defect *vs.* its mass $m_{\rm d}$ for $\gamma = -1$.

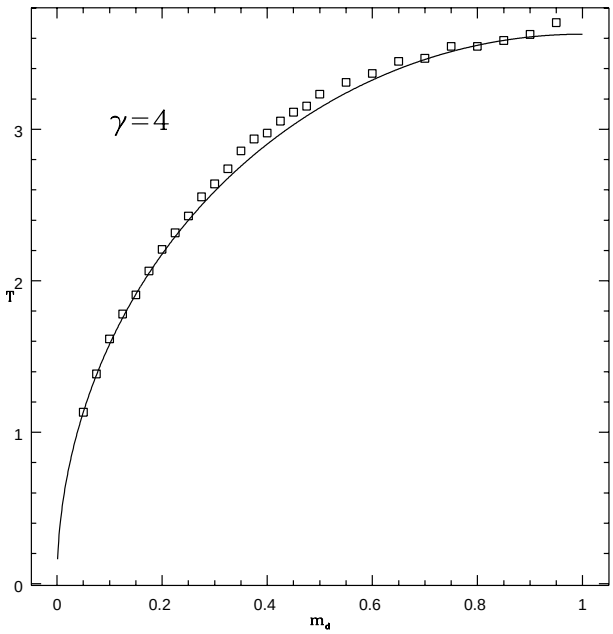

Fig. 6. As in Figure 5, but where now $\gamma = 4$.

In Figures 5–7 we report the experimental data for T compared with those given by (21) for fixed γ *vs.* $m_{\rm d}$.

We remark the existence of a very good agreement between the theoretical predictions and the experimental data.

We notice also that the introduction of the phase ϕ_n in the expression (18) has been the key idea to find the dispersion relation as a function of the defect mass.

Subsequently, we have dealt with the behaviour of the amplitude of the speed of the defect *vs.* $m_{\rm d}$.

For this analysis many numerical experiments have been carried out by varying γ. In particular, we have verified how, independently of the kind of potential used (see (2)), in the plot for the amplitude of the speed in terms of $m_{\rm d}$, two resonance peaks are present in correspondence of the same values $m_{\rm d} \approx 0.15$ and $m_{\rm d} \approx 0.375$. At this stage we observe that the ratio of the frequencies is, approximately, 3/2. Moreover, it seems that a third resonance occurs, although masked by measure errors, for a value of $m_{\rm d} \approx 0.038$, corresponding to a frequency equal to 3 times that of the main resonant mass. To be precise, this third resonance exists without ambiguity for $\gamma = -1$. We have also that the resonance peak relative to $m_{\rm d} \approx 0.15$

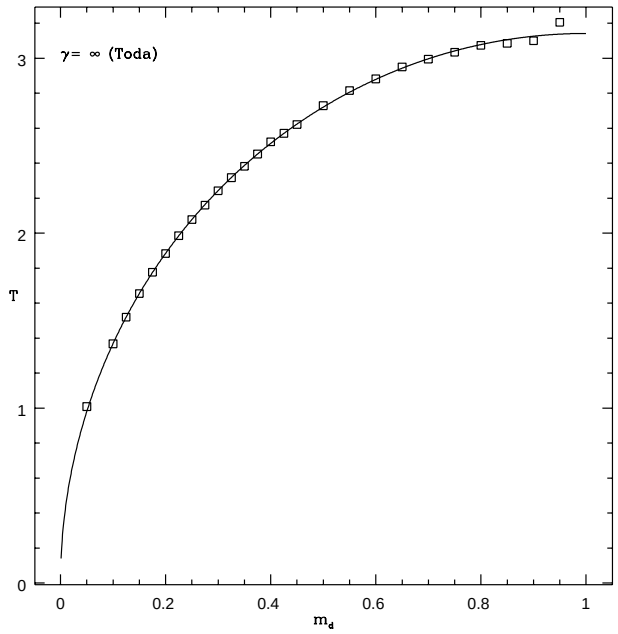

Fig. 7. As in Figure 5, but in the case of Toda potential.

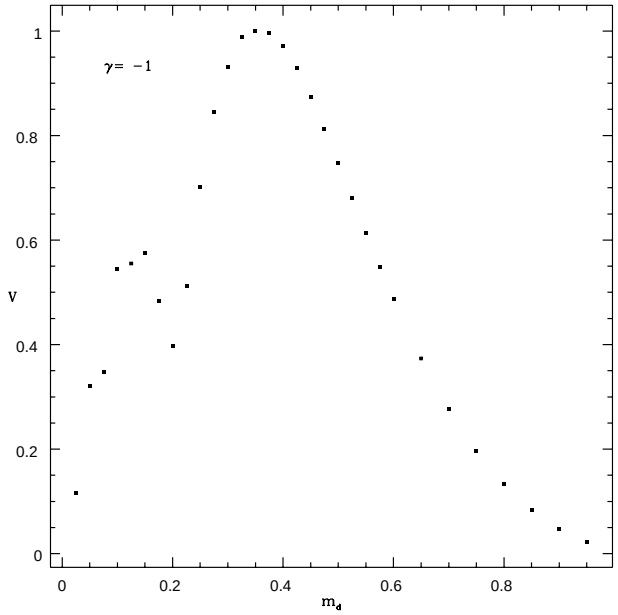

Fig. 8. Behaviour of the amplitude of the defect speed oscillations in terms of the mass $m_{\rm d}$ for $\gamma = -1$. The values of the amplitude have been normalized with respect to its maximum.

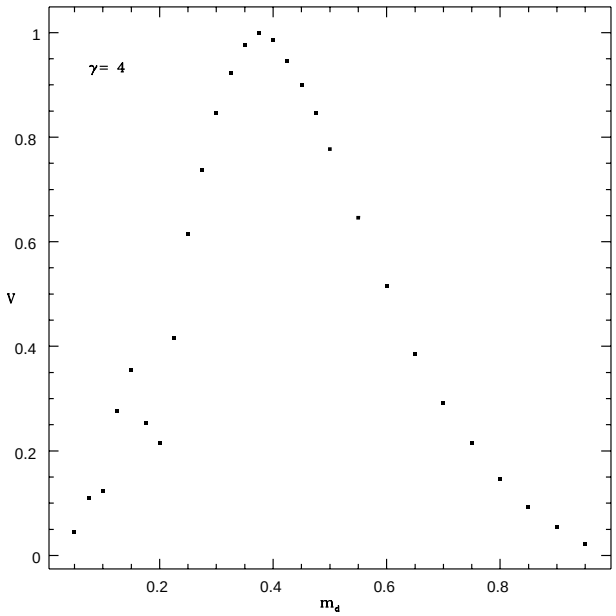

Fig. 9. As in Figure 8, but where now $\gamma = 4$.

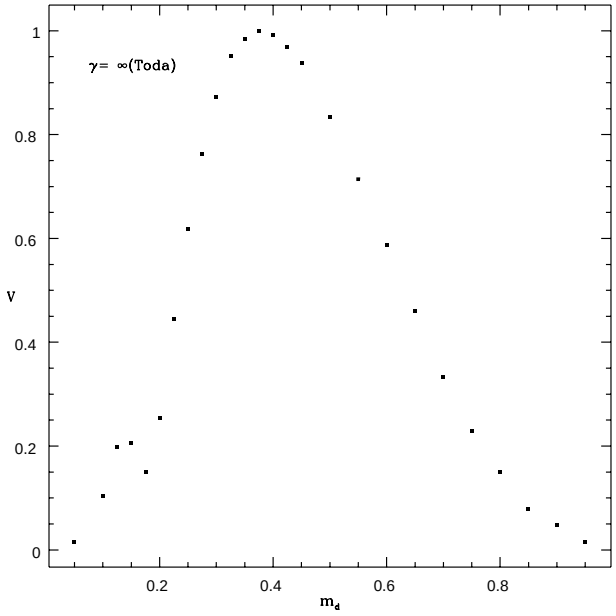

Fig. 10. As in Figure 8, but in the case of Toda potential.

is evident, in our numerical simulations, only starting from values of λ between 1.75 and 2.00. For values of λ less than 1.75, the graph of the speed amplitude in terms of $m_{\rm d}$ seems to exhibit only the main peak in correspondence of $m_{\rm d} \approx 0.375$. A similar result has been achieved in [7].

As an example, in the plots of Figures 8–10 we reproduce, for $\lambda = 2.5$, the experimental data of the amplitude of the defect speed oscillations *vs.* $m_{\rm d}$ for $\gamma = -1$ and $\gamma = 4$, and, for comparison, those of the Toda lattice, which has been studied by means of (3) taking as initial conditions the exact solutions of the Toda lattice itself [10]. Specifically, at $t = 0$ we have chosen

$$y_n = -\sum_{i=n}^{N-1} r_i, \quad \dot{y}_n = 0, \quad \forall n = 2, ..., N-1,$$

where

$$r_n = -\ln(1+\eta_n), \quad \eta_n = \beta^2 \sec h^2(\alpha n - \chi_0).$$

We have taken $\alpha = 1$, $\beta = \sqrt{3}\sinh\alpha$, $\chi_0 = 0.5$.

From the analysis of the plot we argue that the behaviour of the amplitude seems to possess a universality character.

We have tried to interpret such resonances using some models where the results of our numerical experiments might be taken into account. However, our attempts have not succeeded.

In the literature, a search of such effects has essentially failed. Anyway, a hint is contained in [7], where only the main resonance peak is reproduced in formula (2.33), but the effects of the discreteness of the lattice, which may be responsible for the appearing of the other peaks, are not considered. Another attempt is made in [1] (see formulae (2.7–2.11)), where for supersonic kinks the effects of the discreteness of the lattice are taken into account, but the effects induced on the amplitude of the speed of the defect in terms of its mass is ignored. An aspect to be outlined is that the values of the mass of the defect in correspondence of which the amplitude of the speed (and, as well, the amplitude of the corresponding displacement of the equilibrium position y_n) seems to be resonant, remain essentially constant. These values turn out to be independent of the special potential (2) exploited for the interatomic interaction. This situation tells us that owing to the discrete way in which the wave "sees" the lattice, the phenomenon is caused by the strong nonlinear interaction between the solitonic pulse and the defect, rather than by the type of the interatomic interaction.

5 Lattice with two defective atoms

We have examined the binomial lattice in presence of two mass defects. Our simulations have been carried out under the following assumptions.

(i) The number of atoms of the lattice has been brought to 86 for increasing the time of observations, before that the first defected site, $n = 44$, comes into collision with the solitonic pulse reflected on the last atom of the chain.
(ii) The mass m_{d_1} of this first defected atom has been chosen $m_{\mathrm{d}_1} = 0.375$. This value is equal to that corresponding to the maximum of the plot of the amplitude of the defect speed in terms of its mass (see Figs. 8–10) and, therefore, to the minimum of the energy transmitted after the crossing through the site $n = 44$.
(iii) We have taken $\gamma = -1$ in the potential (2).

The aim of this analysis is to see whether in the lattice with a second defective atom, phenomena of resonance similar to those occurring in the case of a single defect may appear. We have investigated numerically the role of the presence of a second defect in terms of the distance δ between the two defective sites. We have found that when $\delta > 5$, for m_{d_2} (the mass of the second defective atom) ranging from 0 and 1, multi-peak resonance phenomena analogous to those relative to the lattice with a single defect are present. This means that the pulse transmitted across the first defected atom has still an energy which is sufficient to excite resonantly a second defect, showing the same resonance peaks in correspondence of the same masses (0.15 and 0.375).

However, for $\delta < 5$ the scenario changes. In particular, among the (not longer harmonic) oscillations of the speeds of the two defective atoms, one notes interference effects which are the more evident, the closer δ is to 1. To make these phenomena manifest, numerical experiments have been performed by taking in turn $m_{\mathrm{d}_2} = 0.05$, 0.375 and 0.85. More specifically, for $m_{\mathrm{d}_2} = 0.05$, an increase of the speed amplitude of the second defect occurs. This amplitude overcomes that relative to the defective atom of mass $m_{\mathrm{d}_1} = 0.375$ in correspondence of the value $\delta = 1$. A similar increase of the amplitude is found for $m_{\mathrm{d}_2} = 0.85$, but the amount of this increase is less than the corresponding one for the amplitude of the speed of the defective atom with mass $m_{\mathrm{d}_1} = 0.375$. The increase of the amplitude for $m_{\mathrm{d}_2} = 0.85$ is followed by a decrease of the amplitude of the speed of m_{d_1}. In the intermediate case, $m_{\mathrm{d}_2} = 0.375$, between the two defects we have observed interference phenomena, although their intensity is not particularly high (apart from a reduction of the amplitudes of the speeds with respect to the situation in which the lattice has a single defect).

A possible explanation of these phenomena, in relation to the three values of the mass of the second defective atom and for $\delta \sim 1$, lies in the fact that the solitonic pulse "sees" the two defects as a unique defect, owing to its size (comparable with the value of the lattice distance) in correspondence of the value $\lambda = 2.5$ employed in the numerical simulation. In practice, when the two defective masses are contiguous, the soliton "sees" them as if these were a single mass, conferring to the latter the same energy that it would have transferred to a single mass of value $m_{\mathrm{d}_1} + m_{\mathrm{d}_2}$. Indeed, for $m_{\mathrm{d}_2} = 0.05$, one has a total mass close to the mass responsible for the main maximum in the curve representing the amplitude of the speed in terms of the mass of the defect. On the contrary, for $m_{\mathrm{d}_1} = 0.85$, which is next to the mass of the non defective atoms of the lattice, we have that m_{d_2} oscillates in opposition of phase with respect to m_{d_1}. In the case $m_{\mathrm{d}_1} = m_{\mathrm{d}_2}$, both amplitudes suffer a considerable reduction in comparison with the case where the defects are far each from the other, as if the soliton should "see" a greater mass, to which a smaller speed amplitude should correspond.

An analysis resembling that previously performed has been considered in [11] in another context, which deals with the behaviour of the transmission coefficient of the solitonic pulse in relation to the interference between defective atoms.

6 Conclusions

We have investigated a class of nearest-neighbour interaction potentials for a one-dimensional chain of atoms. In the continuum limit, the equations of motion of the lattice (called binomial lattice) give rise to a field equation which affords exact solutions of the solitary wave type, used as initial conditions in the treatment of the Cauchy problem of the lattice. These solutions have been distinguished in supersonic and subsonic ones. It turns out that only the supersonic solutions can be employed in the numerical

simulations performed on the lattice. These simulations show that solitonic pulses can propagate in the lattice. Then, we have studied the propagation of waves in the binomial lattice endowed with a defective atom. Precisely, we have considered the interaction of the defect with the solitonic pulse. From the analysis of the amplitude of the defect speed, resonance peaks appear independently of the particular value of the parameter γ (see (2)). There is a strong indication that this phenomenon, which seems new to the best of our knowledge, is due to discreteness effects of the lattice, in the sense that the solitonic pulse moving in the lattice is not able to "see" the lattice as a continuum. In order to interpret the periods of oscillation of the defect, we have described a simple model which is quite compatible with the experimental data of numerical simulations.

Furthermore, to have a confirmation of the occurrence of resonance peaks induced by discreteness effects, we have inserted in the lattice two defective atoms. Also in this case resonance phenomena are found.

Our next programme will be addressed to the study of the thermodynamic properties of the binomial lattice, paying a special attention to the problem of heat conduction and the validity of the Fourier law.

This work was supported in part by PRIN 97 "Sintesi" and by INFN-Sezione di Lecce. The authors thank Prof. Stefano Ruffo of University of Firenze for many helpful discussions.

References

1. M. Peyard, S. Pneumatikos, N. Flytzanis, Physica D **19**, 268 (1986).
2. M. Leo, R.A. Leo, G. Soliani, Phys. Lett. A **60**, 283 (1977).
3. F.D. Tappert, C.M. Varma, Phys. Rev. Lett. **25**, 1108 (1970).
4. L. Casetti, Phys. Scripta **51**, 29 (1995).
5. M. Leo, R.A. Leo, G. Soliani, G. Mancarella, L. Martina, Nuovo Cimento D **1**, 697 (1982).
6. S. Pneumatikos, *in Singularities and Dynamical Systems*, edited by S. Pneumatikos (Elsevier Science Publishers B.V., North-Holland, 1985), p. 397.
7. F. Yoshida, T. Sakuma, Progr. Theor. Phys. **60**, 338 (1978).
8. A. Nakamura, Progr. Theor. Phys. **59**, 1447 (1978).
9. K. Nagahama, N. Yajima, J. Phys. Soc. Jpn **58**, 1539 (1989).
10. M. Toda, Phys. Rep. **18**, 1 (1975).
11. Q. Li, S. Pneumatikos, N. Economou, C.M. Soukoulis, Phys. Rev. B **37**, 3534 (1988).